IGARSS 2023 - 2023 IEEE International Geoscience and Remote Sensing Symposium | 979-8-3503-2010-7/23/$31.00 ©2023 IEEE | DOI: 10.1109/IGARSS52108.2023.10282177

MULTI-FREQUENCY SAR RETRIEVAL OF SEA SURFACE WIND FIELD

F. Nunziata[1], *M. Migliaccio*[1,2], *A. Verlanti*[3], *A. Buono*[1],*E. Ferrentino*[2], *M. Alparone*[1], *S. Zecchetto*[4], *A. Zanchetta*[4], *M. Portabella*[5] and *G. Grieco*[6]

[1] Dipartimento di Ingegneria, Università di Napoli Parthenope, 80143, Naples, Italy
[2] Sezione Osservazione della Terra, Istituto Nazionale di Geofisica e Vulcanologia, 00143, Rome, Italy
[3] Dipartimento di Scienze Chimiche e Geologiche, Università di Cagliari, Cagliari Italy
[4] Istituto di Scienze Polari, Consiglio Nazionale delle Ricerche, 35127, Padua, Italy
[5] Institute of Marine Sciences, 08003, Barcelona, Spain
[6] Istituto di Scienze Marine, Consiglio Nazionale delle Ricerche, 30122, Venice, Italy

ABSTRACT

This study is to present the lesson learned during the activities related to the Italian Space Agency (ASI) funded APPLICAVEMARS project which aims at estimating sea surface wind field from L-, C- and X-band Synthetic Aperture Radar (SAR) imagery. The paper focuses on the X-band results and it describes a new approach to estimate ancillary wind direction info from the SAR image itself using neural networks.

Index Terms— Ocean, Wind field, SAR, NN

1. INTRODUCTION

Sea surface wind field is a parameter of key importance for applications that span from wave forecasting up to storm surge [1]. The microwave scatterometer is specifically designed to deal with ocean wind field retrieval from space and its spatial and temporal sampling meet the requirements of climatological and meso-scale applications.

Nowadays, there is a grat interest towards regional-scale applications and, in particular, to estimate wind field in close basins and in coastal areas. Within this context, the Synthetic Aperture Radar (SAR), i.e., a fine-to-moderate spatial resolution all-day and almost all-weather microwave imaging tool, is of great importance. The SAR provides normalized radar cross section (NRCS) measurements at a spatial resolution finer than the scatterometer one and, therefore, makes possible the wind estimation over coastal areas including semi-enclosed seas, straits, along marginal ice zones and in all that coastal regions where scatterometer measurements are contaminated by land/ice backscatter and the wind vectors are often recognized to be highly variable. In such regions, wind field estimates retrieved from SAR imagery would be very desirable [2, 3].

This study was supported by the ESA-NRSCC cooperation project “Dragon 5”, project ID 57979 - “Monitoring harsh coastal environments and ocean surveillance using radar remote sensing sensors”.

In this study, the main outcomes related to the Italian Space Agency (ASI) funded project APPLICAVEMARS, whose goal is estimating the ocean surface wind vector using L-, C- and X-band SAR imagery, are presented. A wind processor is developed to estimate sea surface wind field from L-band SAOCOM, C-band Sentinel-1A/B and X-band Cosmo SkyMed (CSK) SAR imagery.
In this study, the structure of the X-band wind processor is described and some thoughts experiments are presented. In addition, a novel method to estimate wind direction from the X-band CSK SAR scene is also described that makes use of neural networks (NN). The sensitivity of this method to wind direction is discussed contrateing the wind directions estimated from the X-band SAR scenes with scatterometer ones. Results are very primising a suggest an operational use of this approach when retrieving the wind field on a finer resolution scale.

2. METHODOLOGY

In this section the methodology adopted in this study is presented. First, the Geophysical Model Function (GMF) adopted to retrieve the wind speed is described; then, the approach proposed to estimate wind direction from the features appearing on the SAR image is detailed.
The NRCS, namely σ^0, measured by the SAR for each resolution cell depends on both dielectric and geometric parameters of the sea surface in a way that is not straightforward to invert for wind field retrieval purposes. That is why, typically, a simple semi-emprical formulation is agopted that consists of using a GMF. The latter, typically, includes the NRCS dependance from wind speed u, the relative angle ϕ between the instrument azimuth angle α and wind direction χ, and incidence angle ϑ. In this study, the XMOD2 GMF version, originally derived from X-band TerraSAR-X SAR data, is adapted to CSK SAR measurements [4]. A notable example of GMF is the family of CMOD models which, developed for

$$\sigma^0(u, N, \vartheta) = B_0(u, \vartheta)\left(1 + B_1(u, \vartheta)\cos N + B_2(u, \vartheta)\cos(2N)\right)^{0.625} \quad (1)$$

VV-polarized C-band scatterometers through the collocation between scatterometer data and situ data or model fields, is the key GMF upon which also the XMOD2 is built, see Eq. (1), where $\varphi = \chi - \alpha$. The coefficients B_0 up to B_2 account for the dependency on wind speed and incidence angle (B_0), the upwind-downwind (B_1) and the upwind-crosswind (B_2) effects. The exponent (0.625), first introduced in the fourth version of the CMOD termed as CMOD4, makes sure that higher Fourier terms can be actually neglected in the CMOD formulation.

The SAR is only able to perform one measurement fot each resolution cell. This means that, since there are at least two geophysical parameters (wind speed and direction) modulating SAR measurements, the inversion of winds from SAR data is inherently underdetermined. External wind direction input is, therefore, needed. One possibility relies on the usse of collocated scatterometer measurements which, however, call for an inherently coarser spatial resolution that limts the ability to generate SAR-based wind maps at fine spatial resolution.

It is also well-known wind-induced streaks are often visible in SAR imagery whose orientation is linked to wind direction [5]. Following this rationale several methods have been developed to the estimation of wind direction from SAR scenes: a) the analysis of the orientation of wind-induced streaks, such as boundary layer rolls using Fourier transforms, discrete wavelet transform, continuous wavelet transform [6]. In [7] a deep residual network is used to estimate wind direction from SAR imagery even in small turbulent areas and in absence of streaks on the SAR imagery and in presence of convective turbulence structures, atmospheric Lee waves, and ships. In this study, the latter approach is specialized to the X-band CSK case.

3. WIND PROCESSOR

The schematic that describes the wind processor is depicted in Fig. 1, where wind directions are estimated from both the SAR image itself (using a NN approach) and external sources (e.g., scatterometer measurements, or atmospheric model outputs) and the wind speeds is estimated using the XMOD2 adapted for the CSK case..

The processing scheme can be described as follows:

- The VV-polarized ground-detected and geocoded (GEC) CSK SAR image is ingested in the processing chain.
- The ingested image is preprocessed to perform calibration, down-sampling and land masking.
- A cost function is implemented that consists of minimizing the difference between the measured NRCS and the one predicted by the XMOD2 GMF.

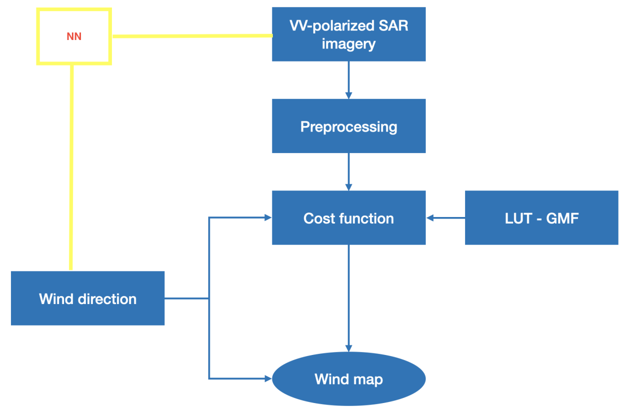

Fig. 1. Schematic of wind retrieval by CSK SAR imagery,

The cost function includes:

- The GMF stored as a look-up-table (LUT).
- The wind direction information that comes from both external sources, i. e., collocated scatterometer measurements and ECMWF data, and the SAR image itself

4. DATA SET

The SAR data set consists of 54 CSK SAR scenes, collected in North Sea with collocated Advanced Scatterometer (ASCAT) and ECMWF re-analysis winds. They result from sorting out SAR data corrupted by rain or presenting processing artifacts. A premium subset constisting of 19 CSK SAR scenes whose time collocation with ASCAT is no larger than 90 minutes is also considered to perform a sensitivity analysis of NN approaches to wind direction.

5. EXPERIMENTS

In this section, experimental results related to the processing of the X-band SAR scenes are presented. A first experiment is undertaken to analyze the CSK wind speed retrieval capabilities based on the adapted XMOD2 with respect to ASCAT collocations, while a second experiment is performed to investigate the sensitivity of NN techniques for wind direction estimation purposes.

The scatterplot of Fig. 2 (a) points out that most of the datapoints that contribute to broadening the scatterplot call for larger delays with the correspondent ASCAT acquisition (between 60 and 90 minutes). In addition, some well-collocated

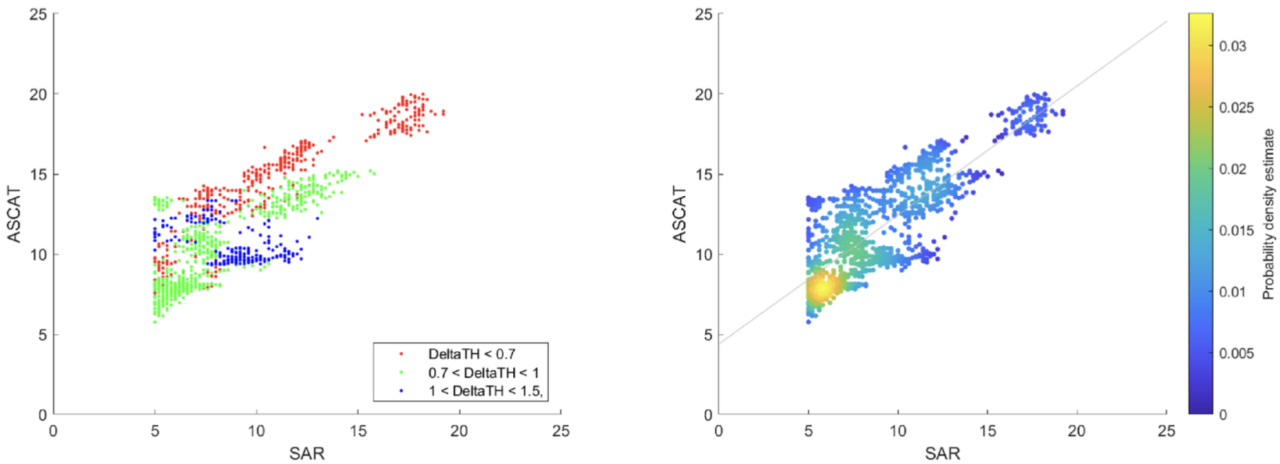

Fig. 2. Scatterplot that contrasts CSK wind retrievals carried on the premium data set with ASCAT. The time lag between CSK and ASCAT is marked using different colors (a) and the datapoints are clustered according to their occurrence probability (b).

datapoints (the red one) result in a large deviation at low wind speed. Hence, the low wind speeds are not well retrieved by CSK. The density plot of Fig. 2 (b) points out that datapoints are very clustered. This means that the available dataset is not uniform in terms of wind speed.

With reference to the second experiment, each of the 19 CSK SAR images are first partitioned into square boxes whose size matches the scatterometer pixel one, i. e., 10 km. Then, data augmentation is performed to this SAR data set which consists of rotating each box of 90°, 180° and 270°. The labels are discretized with a granularity of 10 units and the outliers are sorted out. As a result, a dataset consisting of 6608 images is inputted to NNs, which are split into about 85% for training, 10% for validation and 5% for testing. Among convolutional NNs (CNNs), the ResNet-18 architecture is selected that, belonging to the ResNet CNN family, is found to provide the best performance. The performance of the ResNet-18 is also contrasted with a state-of-the-art CNN, the Inception v3 architecture.
ResNet and Inception CNN families call for two completely different paradigms: the former allows increasing the number of layers; while the latter allows increasing the number of convolution per layer. Nonetheless, no significant difference in terms of performance is observed, even though ResNet-18 calls for faster training than Inception v3. Hence, a joint use of the two CNN stategies is considered by exploiting the Inception ResNet v2 CNN, which outperforms ResNet-18 and Inception v3 configuratio achieving a 96% accuracy. Experimental results relevant to the confusion matrix are shown in Fig. 3.

6. CONCLUSIONS

This study presents the main results relevant to the ASI funded APPLICAVEMARS project, whose aim is to estimate sea surface wind field from L-, C- and X-band SAR imagery. The paper focuses on the X-band results obtained from a premium CSK SAR data set, also presenting a new CNN-based approach to estimate ancillary wind direction from the SAR image itself. Experiments show promising results in wind speed retrieval accuracy using a GMF approach adapted from XMOD2 and in wind direction estimation using the Inception ResNet v2 CNN.

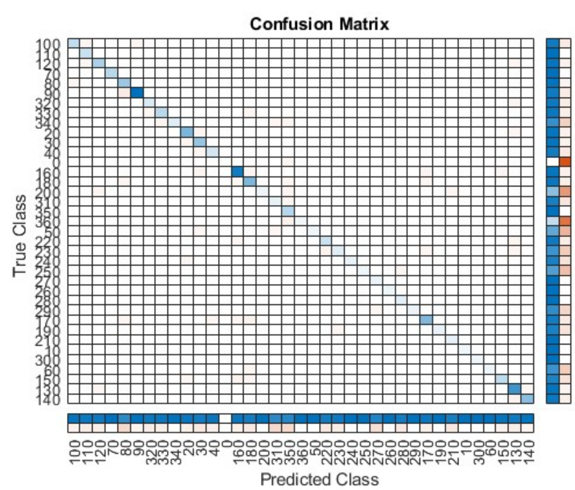

Fig. 3. NN sensitivity to wind direction: confusion matrix.

7. ACKNOWLEDGEMENTS

The authors would thank ASI for providing the CSK SAR data set under the APPLICAVEMARS project, contract 2021-4-U.0 (CUP F65F21000070005).

8. REFERENCES

[1] D. B. Chelton, M. G. Schlax, M. H. Freilich, and R. F. Milliff, “Satellite measurements reveal persistent small-scale features in ocean winds,” *Science*, vol. 303, no. 5660, pp. 978–983, 2004.

[2] G. Benassai, A. Montuori, M. Migliaccio, and F. Nunziata, “Sea wave modeling with X-band COSMO-SkyMed© SAR-derived wind field forcing and applications in coastal vulnerability assessment,” *Ocean Science*, vol. 9, no. 2, pp. 325–341, 2013.

[3] G. Benassai, D. Di Luccio, V. Corcione, F. Nunziata, and M. Migliaccio, “Marine spatial planning using high resolution SAR measurements,” *IEEE Journal of Oceanic Engineering*, vol. 3, no. 43, pp. 586–594, 2018.

[4] X. Li and S. Lenher, “Algorithm for sea surface wind retrieval from TerraSAR-X and TanDEM-X data,” *IEEE Transactions on Geoscience and Remote Sensing*, vol. 52, no. 8, p. 2928–2939, 2014.

[5] C. Wackerman, C. Rufenach, R. Shuchman, J. Johannessen, and K. Davidson, “Wind vector retrieval using ERS-1 synthetic aperture radar imagery,” *IEEE Transactions on Geoscience and Remote Sensing*, vol. 34, no. 6, pp. 1343–1352, 1996.

[6] S. Zecchetto, F. De Biasio, A. Della Valle, G. Quattrocchi, E. Cadau, and A. Cucco, “Wind fields from C and X band SAR images at VV polarization in coastal area (Gulf of Oristano, Italy),” *IEEE Journal of Selected Topics in Applied Earth Observations and Remote Sensing*, vol. 9, no. 6, pp. 325–341, 2016.

[7] A. Zanchetta and S. Zecchetto, “Wind direction retrieval from Sentinel-1 SAR images using ResNet,” *Remote Sensing of Environment*, vol. 253, p. 112178, 2021.